Article

Not peer-reviewed version

Combustion Control of Ship's Oil-Fired Boilers based on Prediction of Flame Images

Chang-Min Lee *

Posted Date: 26 July 2024

doi: 10.20944/preprints202407.2201.v1

Keywords: Combustion control; Emission prediction; IMC-based PI Control; Real-Time Control; Performance assessment

Article

Combustion Control of Ship's Oil-Fired Boilers based on Prediction of Flame Images

Chang-Min Lee

Division of Marine System Engineering, Korea Maritime and Ocean University, 727, Taejong-ro, Yeongdo-gu, Busan 49112, Korea; Korea Maritime & Ocean University; oldbay@kmou.ac.kr

Abstract: This study proposes and validates a novel combustion control system for Oil-Fired Boilers aimed at reducing air pollutant emissions through flame image prediction. The proposed system is easily applicable to existing ships. Traditional proportional combustion control systems supply fuel and air at fixed ratios according to the set steam load, without considering the emission of air pollutants. To address this, a stable and immediate control system is proposed, which adjusts the air supply to modify the combustion state. The combustion control system utilizes oxygen concentration predictions from flame images via SEF+SVM as control inputs, and applies Internal Model Control (IMC)-based Proportional-Integral (PI) control for real-time combustion control. Due to the complexity of modeling the image-based system, IMC parameter tuning through experimentation is essential for achieving effective control performance. Experiments conducted on a 3000 kg/h marine oil-fired boiler in actual operation optimized the controller parameters for stability and responsiveness, and validated their effectiveness. The results demonstrate the potential of the proposed system to improve combustion efficiency and reduce emissions of air pollutants. This study provides a feasible and effective solution for enhancing the environmental performance of marine oil-fired boilers. Given its ease of application to existing ships, it is expected to contribute to sustainable air pollution reduction across the maritime environment.

Keywords: combustion control; emission prediction; IMC-based PI Control; real-time control; performance assessment

1. Introduction

Combustion boilers are widely used for steam generation in marine industries, power plants, and various utilities requiring substantial thermal energy[1]. In the marine sector, although the trend of producing steam-powered ships has significantly declined [2], boilers burning diesel fuel are still extensively used on ships employing diesel engines as the primary propulsion system. However, fossil fuels like diesel contribute to global warming by emitting greenhouse gases such as NO_x, SO_x, and CO2 during combustion [3,4]. Compared to main propulsion systems such as internal combustion engines, there is relatively less regulation and concern regarding pollutants emitted from combustion boilers [5,6]. Therefore, efforts are needed to reduce air pollutants generated from the exhaust gases of ship boilers.

The boiler system generates exhaust gases with thermal energy through the atomization and combustion of pressurized air and fuel. These exhaust gases convert water into steam via heat transfer surfaces such as water tubes or fire tubes. The amount of air pollutants emitted varies depending on the equivalence ratio, which is the ratio of fuel to air during the combustion process [7].

To reduce air pollutants, it is necessary to properly control the air and fuel supplied for combustion [8]. However, traditional boiler combustion systems use a proportional combustion control, where the load of steam is the control target, and predetermined fuel and air flow rates are supplied for combustion. This method ensures system stability but does not take air pollutant

 doi:10.20944/preprints202407.2201.v1

emissions into account [9]. Consequently, research has been continuously conducted to directly control the fuel oil and air flow rates supplied to the combustion system in order to reduce air pollutants [10,11].

However, although these control solutions have proven effective in reducing air pollutant emissions, they need to be designed at the manufacturing stages, leading to increased initial and operational costs. Additionally, advanced control methods requiring high accuracy in system modeling can cause combustion instability and flame extinction due to transient responses when directly applied to the dynamic boiler systems sensitive to environmental changes [12]. These challenges related to cost and stability continue to support the widespread use of traditional proportional combustion control.

Therefore, this study proposes a system that reduces emissions of air pollutant by adding a control system for combustion optimization to the existing Oil-Fired Boiler (OFB) combustion system, which ensures system stability.

In existing research, air pollutants and oxygen concentration were used as inputs through either direct measurement or indirect estimation based on operational data [13–15]. However, the direct measurement method using devices is not suitable for real-time control due to the delay between the combustion control point and the measurement point [16]. Additionally, the indirect measurement method based on operational data is economically disadvantageous as it requires numerous data collection devices, and the loss of a single operational data point or sensor failure can significantly impact prediction accuracy, leading to errors in control inputs [14]. Consequently, research on control systems using soft measurement has been continuously conducted.

In this study, a soft measurement method is employed by observing quasi-instantaneous flame images to predict air pollutants, using these predictions as control inputs to achieve real-time control.

It is challenging to mathematically represent the dynamic modeling of a boiler combustion system utilizing flame images as control inputs. Therefore, machine learning-based modeling methods using operational data are frequently employed for such complex systems [17]. To effectively control the modeled system, selecting appropriate control techniques and parameters is crucial [18].

In this study, an IMC-based PI controller is used to maintain the oxygen concentration derived from flame images at a constant level. PI control is a well-established method in numerous industrial processes, and by incorporating the robustness of IMC, it provides a simple yet highly reliable solution. This makes it readily applicable to ships, easy to operate, and capable of delivering excellent performance [19,20].

The experiments were conducted on a 3000 kg/h heavy oil boiler currently in use at the site. To predict the oxygen concentration, an indirect measure of air pollutant emissions and combustion efficiency, the SEF+SVM method was used to extract features from flame images and make predictions.

This method was validated in prior research conducted on the same plant. Flame images under six different combustion conditions were collected, and a trained model of oxygen concentration estimation was established as the control input for the control system to form a closed-loop. The transfer function of the configured closed-loop was estimated using input-output data from experiments, and an IMC-based PI controller was designed accordingly. The parameters of the IMC were optimized through experiments to balance robustness and control performance, and their effectiveness was demonstrated through control performance verification.

The objectives of this study can be summarized as follows:

1. Propose a combustion control system to reduce air pollutant emissions from marine Oil-Fired Boilers.
2. Develop a real-time combustion control system using predicted oxygen concentration from flame images as control inputs.
3. Tune an IMC-based PI controller through experiments to compensate for system discrepancies.

 doi:10.20944/preprints202407.2201.v1

2. Combustion Control System for Marine Oil-Fired Boilers

Figure 1 shows a schematic diagram of the experimental setup. The OFB on the ship operates as a closed-loop control process, $\mathcal{P}1$, to reach the set steam pressure. This process adjusts the fuel valve and the damper opening of the turbocharger fan at a fixed ratio according to the internal logic programmed into the PLC to achieve the set control target. In this process, the combustion state cannot be independently adjusted in response to disturbances such as fuel oil properties or system variations, as the fuel supply and air supply cannot be controlled separately. To address this issue in the existing OFB system and improve the combustion state, a new control process, $\mathcal{P}2$, is proposed, which includes an additional servo motor for damper adjustment controlled by $\mathcal{P}1$, as shown in Figure 1.

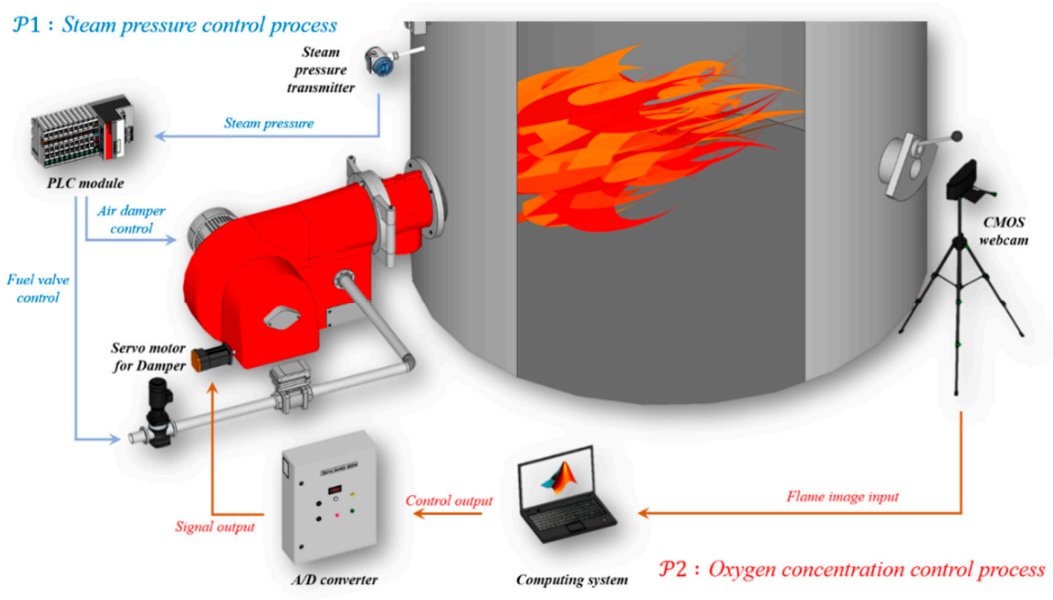

Figure 1. Schematic of Boiler Combustion Experiment.

The $\mathcal{P}2$ control process predicts the combustion state from flame images and adjusts the servo motor to regulate the air supply based on this feedback.

Combustion parameters such as SO_x, NO_x, CO_2, and CO, as well as oxygen, included in the exhaust gases can be easily measured using gas analyzers. However, the measured exhaust gas values in this method have a delay time due to the process of flowing from the combustion point to the measurement point. This delay tends to cause the feedback control loop, which regulates oxygen concentration, to overcompensate for errors, resulting in slower control response and larger transient responses. In contrast, using flame images, which are indicators of quasi-instantaneous combustion states, as inputs for oxygen measurement allows for immediate reflection of the current combustion state, enabling real-time continuous flame control. A 1920×1080 pixel CMOS webcam is used to collect high-resolution flame images. The camera is positioned at the flame observation port on the side of the boiler in accordance with SOLAS regulations. The collected flame images are transmitted to a computer via a USB 3.0 interface, and the predicted values of oxygen concentration, obtained from a pre-trained model, are used as feedback signals in the control system.

The error in the oxygen concentration setpoint is converted into a control signal for the air regulation damper through the designed controller. In the $\mathcal{P}1$ control system, fuel and air are controlled simultaneously at a fixed ratio according to the steam load. In contrast, the proposed $\mathcal{P}2$ control system adjusts the damper opening, which regulates the air supply, independently, thereby allowing control over the combustion state. To achieve individual damper control, an A/D converter drive is used to convert the analog control output to an angle ranging from 0 to 90 degrees, and a servo motor is installed at the end of the damper to control it in real-time.

 doi:10.20944/preprints202407.2201.v1

To train the prediction model of oxygen concentration for the experimental OFB and to compare and verify the effectiveness of the control system, information on air pollutants is automatically recorded in the computing system via an exhaust gas analyzer from the funnel during the process. Specifically, the oxygen concentration, which is an indirect measure of energy consumption and combustion state as well as the control target, is recorded as time-series data along with the flame images.

3. Oxygen Concentration Estimation Model Using Saturation Extraction Filter

To estimate the control input, specifically the oxygen concentration, in real-time, flame images representing quasi-instantaneous combustion states are processed through the SEF-SVM model. This model extracts linear features from the flame images, focusing on saturation information, and converts these features into histograms to predict exhaust gas information in real-time.

The effectiveness of the SEF-SVM model was validated through experiments conducted on the same ship's OFB plant. The model demonstrated an R^2 value of 0.97 in oxygen concentration measurement performance. Furthermore, the measurement delay time was reduced to an average of 2.1 seconds, confirming its suitability for use as an input in real-time control [21].

Figure 2 shows a schematic diagram of the SEF-SVM model.

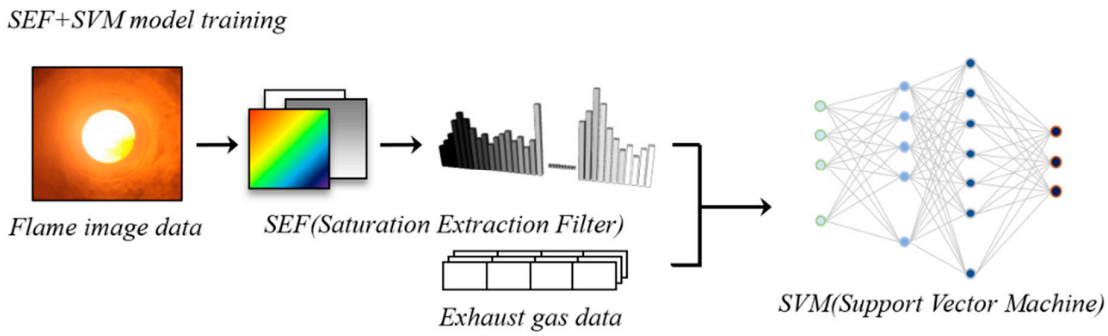

Figure 2. Learning Structure of Flame Images Using SEF+SVM.

The collection of flame images utilizes the existing flame observation port, which presents a limitation in capturing the full size and shape of the flame. To mitigate this, the images are resized to 800×820 pixels to capture the reflective light from the wall surface of the observation port. This size was determined to be appropriate for the OFB through experimentation, ensuring that the histogram can accurately represent the data without exceeding 2 bytes per bin (216 bytes).

The collected flame images are initially captured in RGB format and then converted to HSV format. From this, only the Saturation component, which exhibits linear characteristics corresponding to different combustion states, is extracted. By histogramming this information, the original 800(H)×820(W)×3×2 byte data is reduced to a 256×2 byte feature-extracted dataset. This reduced dataset is then combined with the corresponding time-series exhaust gas data and used for regression training in the SVM model.

3.1. Data Collection

Figure 3 presents the data collection process used in the experiment.

 doi:10.20944/preprints202407.2201.v1

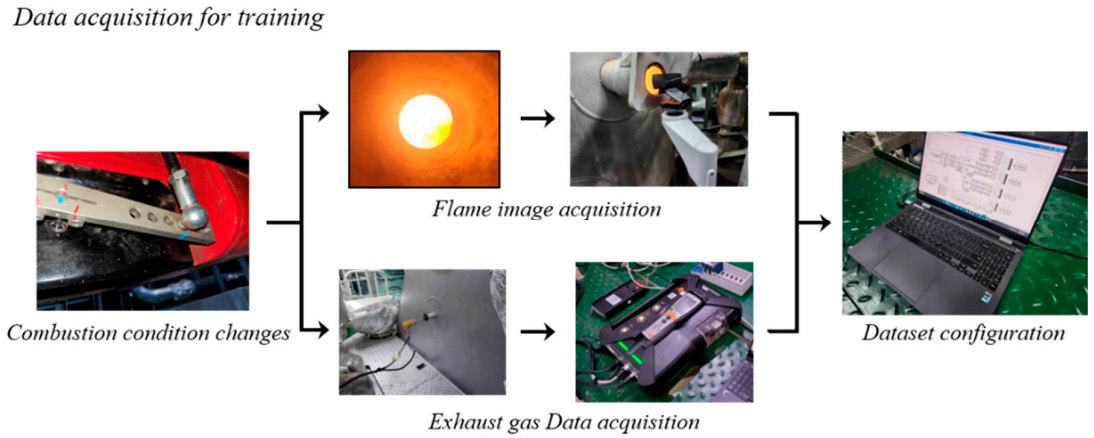

Figure 3. Data Acquisition Process of Flame Images and Exhaust Gas Data.

During the data collection process, the combustion environment is divided into six distinct stages. For each stage, 200 data points are collected, resulting in a total of 1,200 time-series data points.

The combustion environment is manually controlled by operating the OFB while maintaining a constant supply of fuel and air, disregarding the steam pressure in the $\mathcal{P}1$ control system. In this state, as shown in Figure 3, the amount of supplied air is varied by adjusting the control hole installed on the linkage of the air damper. Changes in the air supply affect the oxygen concentration δ_o in Equation 1, fuel-lean equation, altering the Combustion Equivalence Ratio (CER) and consequently changing the exhaust gas composition due to variations in C, H, and N reacting in the fuel [7]. Therefore, as the CER increases, the peak value of the saturation in the flame image changes. The data on air pollutants and oxygen concentration in the exhaust gas are stored as time-series data synchronized with the SEF-processed data, forming the dataset.

$$\varphi = \frac{\rho_e}{\rho_a} = 18.5\left(\frac{13\delta_o + 37}{2 - 9.52\delta_o}\right)^{-1} \quad (1)$$

3.2. Training of the Prediction Model of Oxygen Concentration

The flame images and oxygen concentration data, stored from the process, are used to train a linear regression model for predicting oxygen concentration. The training model employs SEF+SVM, identical to model E1 trained with 300 samples in previous research, and uses a training dataset of 1,200 data points, with 200 samples for each environmental variation. While increasing the dataset size improves the model's performance by increasing the learning rate and reliability, it also raises the risk of overfitting, so the dataset size must be appropriately selected through experimentation. The training results for the new prediction model E2 are shown in Table 1. The evaluation metrics indicate the R^2 of 0.976, RMSE of 0.1159, and MAE of 0.1159. Compared to the proven performance of SEF+SVM, the R^2 increased by 0.62%, while the RMSE and MAE decreased by 31.74% and 4.45%, respectively, confirming the effectiveness of the E2 prediction model.

Table 1. Learning Results of Predictive Models E1 and E2.

Prediction Model	Training Dataset	R^2	RMSE	MAE
E1	300	0.97	0.1698	0.1213
E2	1200	0.984	0.1159	0.1159

 doi:10.20944/preprints202407.2201.v1

4. Development of an IMC-PID Based Oxygen Concentration Control System Using Flame Images

By utilizing flame images as input for oxygen concentration, the input delay issues associated with oxygen concentration meters can be resolved, allowing for the establishment of a real-time control system to regulate the oxygen concentration in the exhaust gases of the OFB. The schematic diagram of the control system $S2$ for $\mathcal{P}1$ proposed in this study is shown in Figure 4.

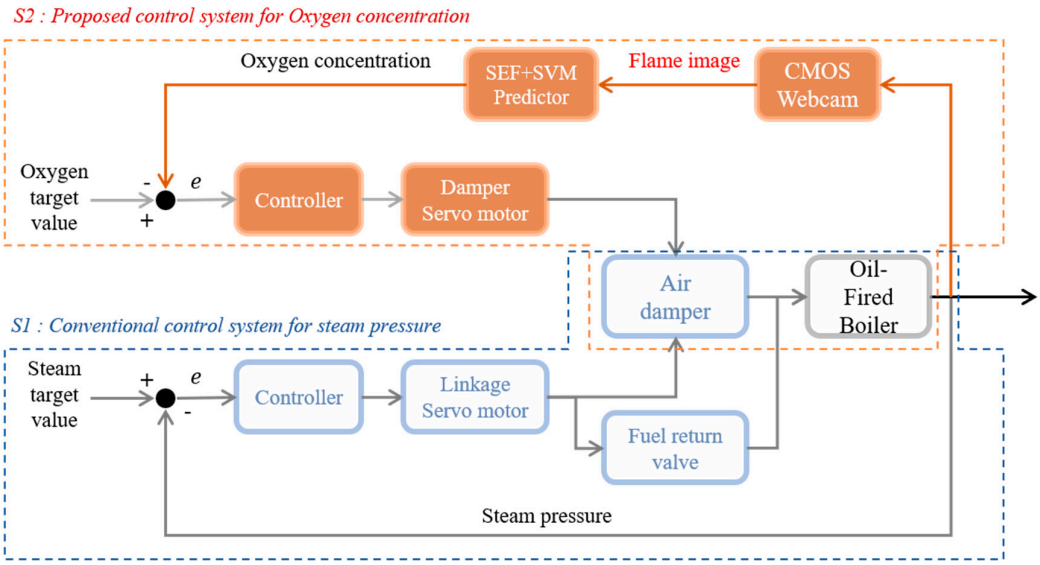

Figure 4. Overall of the Boiler Control System with the Proposed Combustion Control System.

$S1$ is the existing control system used for boiler combustion. This system is a proportional combustion control system that simultaneously controls the air flow and fuel quantity to maintain constant steam pressure. Since this ratio is set by the manufacturer during the commissioning part with a primary focus on combustion stability, the flame remains stable despite changes in the environmental conditions of the supplied air and the characteristics of the fuel. However, the emissions of air pollutants vary as a result. Consequently, by adjusting the amount of supplied air while maintaining a constant fuel quantity, it is possible to control the emissions of air pollutants while ensuring combustion stability during the stable combustion process of the flame.

Therefore, this study proposes an oxygen concentration control system, $S2$, that can additionally control the air damper opening, which is proportionally controlled in the existing $S1$ system. The control system uses flame images as real-time input to predict oxygen concentration through the SEF+SVM predictor. The predicted oxygen concentration is then used to adjust a servo motor for the damper via a controller, compensating for any deviation from the target value. This controlled damper alters the amount of air supplied to the combustor, thereby controlling the air pollutants generated during the combustion process.

4.1. Setting Control Objectives

The air pollutants emitted from the OFB are inversely proportional to the amount of air supplied because the amount of oxygen reacting with the fuel components increases during lean combustion when the equivalence ratio is less than 1. Maintaining the oxygen concentration in the exhaust gases is crucial to minimize soot particles and black smoke while effectively controlling cooling losses due to heat release and nitrogen oxide (NO_x) emissions. Therefore, setting and maintaining an optimal oxygen concentration is essential for the effective control of air pollutants.

Additionally, previous studies using the same type of boiler as the OFB employed in this research have shown that the air pollutants CO_2, NO_x, and SO_2 tend to be inversely proportional to oxygen concentration in the exhaust gases. Moreover, excessive supercharging should be avoided, as

 doi:10.20944/preprints202407.2201.v1

it can reduce combustion efficiency due to heat loss in the exhaust gases. Therefore, it is crucial not to maintain the oxygen concentration excessively low [22].

The previous studies analyzing the exhaust gas characteristics of boiler systems based on oxygen concentration have demonstrated similar tendencies and highlighted the importance of maintaining an appropriate oxygen concentration.

In the study by J. Chen et al., the exhaust gas oxygen concentration of a coal-fired boiler was adjusted between 2% and 5%, revealing a correlation between oxygen concentration and NO_X emissions. Additionally, the study examined the impact of soot and graphite on flame image measurements with varying oxygen concentrations. It was found that at an oxygen concentration of 4.02%, the occurrence of soot and graphite was minimized, resulting in the least noise in flame image recognition [23].

The study conducted by G. Xiao et al. on gas-fired boiler combustion examined the correlation between heat release and NO_X production in boilers. The study established weightings for heat release and NO_X production, finding that to double the weighting for reducing NO_X emissions, the oxygen concentration needs to be increased by approximately 1.14 times under various load conditions. In this research, an oxygen concentration of 3.5% achieved a 1:1 balance between heat release and NO_X production at 80% load. When adjusting the weighting to reduce NO_X production, the optimal oxygen concentration was found to be around 4.0% [24].

Based on a comprehensive review of the exhaust gas characteristics of the target ship's OFB and related researches, this study concludes that setting the control target value for the oxygen concentration in the exhaust gas to 4% is appropriate for real-time combustion control of the boiler.

4.2. Estimation of Transfer Function Based on Step Response

To set the controller, the transfer function of the control system must first be determined. Although classical methods such as calculating differential equations can be used to find the transfer function, this approach is not straightforward for the given system due to the numerous variables, including changes in the supplied air, fuel characteristics, and heat transfer efficiency variations with load. Therefore, this study employs a method that identifies the system by providing a constant input and analyzing the resulting response. This method is well-suited for irregular and non-linear systems, and it offers the advantage of being able to adapt to the desired model structure despite the presence of many system variables by using actual data [17,25].

To identify the system, the combustion control system $S1$ is maintained at a load of 78%, ensuring that the oxygen concentration in the exhaust gas remains at 4% while fuel is supplied at a constant rate. During this process, a step input of +5 degrees in the open direction is applied to the servo motor of $S2$, and the oxygen concentration, as inputted through flame images, is recorded. Figure 5 shows the oxygen concentration output of the system in response to the step input.

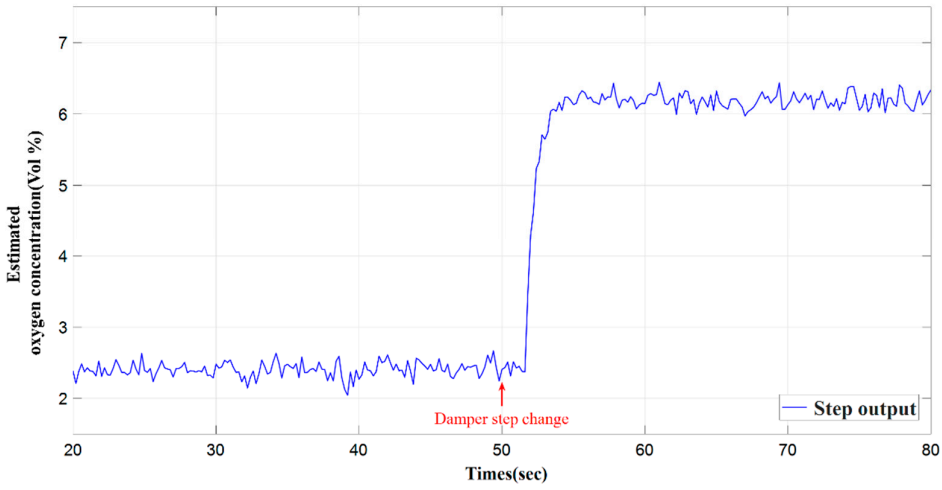

Figure 5. Concentration of O_2 Change in Response to Servo Angle Step Input.

 doi:10.20944/preprints202407.2201.v1

The collected data is then used to estimate the transfer function using MATLAB's System Identification Toolbox. This method utilizes machine learning algorithms to estimate the transfer function through the learning of input and output data. The order of the system is specified from first to third order, and the transfer functions are estimated as shown in Table 2.

Table 2. Transfer Function Estimation through Training of Machine Learning Algorithms.

system order	Estimated Numerator	Estimated Denominator	Fit Rate to Data	MSE
1	0.2187	1, 2648.14	81.47	0.124
2	0.2187, 0.5960	1, 2847.82, 1508.78	99.28%	0.0001833
3	2.867, 0.05036	1, 44.45, 97.21, 0.0841	90.51%	0.03482

The accuracy presented in Table 2 confirms that a second-order system is most suitable. This indicates that the fuel is consistently supplied, and disturbances other than changes in the air supply do not significantly affect the system. Therefore, the system transfer function is designated as $\bar{\mathcal{G}}_{S2}$ in Equation 2, and a controller is designed accordingly.

$$\bar{\mathcal{G}}_{S2} = \frac{0.2187s + 0.5960}{s^2 + 2847.82s + 1508.78} = \frac{0.2187(s + 2.728)}{(s + 0.523)(s + 2847.29)} \quad (2)$$

Examining the poles and zeros of the transfer function $\bar{\mathcal{G}}_{S2}$, the poles are located at $s1 \approx -0.523, s2 \approx -2847.29$. Since the real parts of both poles are negative, they are positioned on the left half of the complex plane, indicating that the system is stable and controllable. The zeros are also real and negative, which confirms that they do not affect the system's stability

4.3. Tuning of the IMC-Based PI Controller

To effectively control the image-based combustion system of the $S2$ system, it is essential to employ an appropriate controller. This experiment utilizes an IMC-based PI controller for system regulation. Given that the $S2$ system uses flame images as input signals, high-frequency noise may arise from intermittent prediction errors. In such cases, the derivative component of a PID controller could amplify the noise, making a PI controller more suitable [18]. Furthermore, for the sake of computational simplicity in tuning the IMC controller, a PI controller is used.

Figure 6 shows the closed-loop structure of the IMC applied to the actual system transfer function $\mathcal{G}_{S2}$.

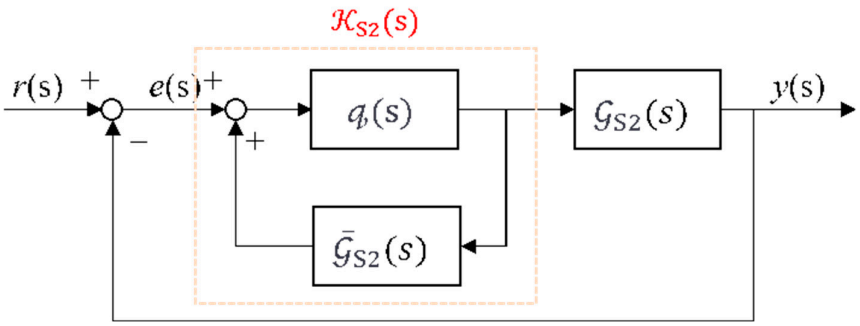

Figure 6. Control Diagram of IMC.

$\bar{\mathcal{G}}_{S2}$ is the internal model transfer function estimated from the data, $q(s)$ is the IMC controller, and $\mathcal{K}_{S2}(s)$ is the controller integrated with the internal model. As determined in **Section 4-2**, $\bar{\mathcal{G}}_{S2}$ is a second-order function and can be expressed as shown in Equation 3.

$$\bar{\mathcal{G}}_{S2}(s) = \frac{k_p(\beta s + 1)}{(\tau_a s + 1)(\tau_b s + 1)} \ (\tau_a < \tau_b) \quad (3)$$

 doi:10.20944/preprints202407.2201.v1

The τ_a *and* τ_b are the time constants of the system, k_p is the proportional gain, and β is the constant associated with the zero. Consequently, the IMC controller can be expressed as shown in Equation 4, where $f(s)$ represents the IMC filter. The filter function $f(s)$ is set as a second-order system, corresponding to the order of the internal model, and λ is the filter constant that defines the trade-off between control performance and robustness.

$$q(s) = \bar{G}_{S2}^{-1} f(s) \tag{4-1}$$

$$f(s) = \frac{s+1}{(\lambda s+1)^2} \tag{4-2}$$

By standardizing the closed-loop structure using this approach, the IMC controller $q(s)$ and the internal model $\bar{G}_{S2}$ can be integrated to form the classic controller $\mathcal{K}_{S2}(s)$. This can be expanded using Equation (4-1) and Equation (4-2) to be expressed in the form shown in Equation 5.

$$\mathcal{K}_{S2}(s) = \frac{q(s)}{1-\bar{G}_{S2}q(s)} = \frac{\bar{G}_{S2}^{-1} f(s)}{1-\bar{G}_{S2}\bar{G}_{S2}^{-1} f(s)} \tag{5-1}$$

$$\mathcal{K}_{S2}(s) = \frac{\tau_b}{k_p\lambda}\left(1+\frac{1}{\tau_b s}\right)\frac{(\tau_a s+1)}{(\beta s+1)} = \frac{\tau_b}{k_p\lambda}\left(1+\frac{1}{\tau_b s}\right) f_l(s) \tag{5-2}$$

The expanded Equation (5-2) shows that $\mathcal{K}_{S2}(s)$ takes the form of a PI controller. The term $\frac{(\tau_a s+1)}{(\beta s+1)}$ can be considered as a lead-lag filter and is denoted $f_l(s)$. The classic controller is expressed as $\mathcal{K}_{S2}{}'(s)$ in Equation 6, using the proportional gain K_p and the integral gain K_i.

$$\mathcal{K}'_{S2}(s) = \frac{\tau_b}{k_p\lambda}\left(1+\frac{1}{\tau_b s}\right) = K_p\left(1+\frac{K_i}{s}\right) \tag{6}$$

Figure 7 shows the final form of the closed-loop control system for $S2$.

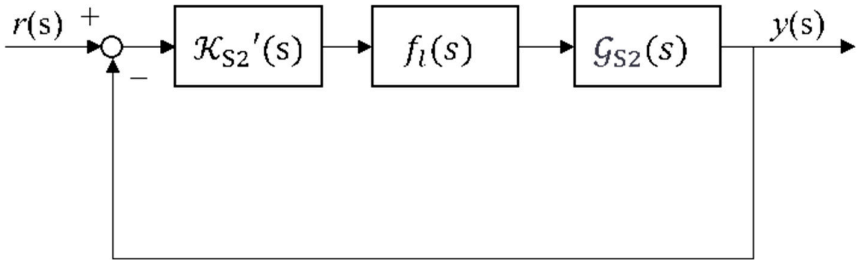

Figure 7. Final Form of IMC Control Diagram of a Two-State System.

Therefore, the IMC-based PI controller $\mathcal{K}'_{S2}(s)$ can be expressed as a function of the proportional gain K_p and the integral gain K_i with respect to λ, as shown in Equation 7.

$$K_p = \frac{\tau_b}{k_p\lambda}, \; K_i = \frac{1}{k_p\lambda} \tag{7}$$

The control elements for system $\boldsymbol{S2}$ are summarized in Table 3.

Table 3. Control Elements of the System.

$\bar{G}_{S2}(s)$	$f(s)$	$\mathcal{K}'_{S2}(s)$	K_p	K_i
$\frac{k_p(\beta s+1)}{(\tau_a s+1)(\tau_b s+1)}$	$\frac{s+1}{(\lambda s+1)^2}$	$K_p\left(1+\frac{K_i}{s}\right)$	$\frac{\tau_b}{k_p\lambda}$	$\frac{1}{k_p\lambda}$
k_p= 2.1865704, β = 2.728423e3, τ_a= 3.51e−4, τ_b= 1.887649				

 doi:10.20944/preprints202407.2201.v1

5. Case Study

5.1. Example Case

By installing an IMC-based PI controller in the $S2$ combustion control system and specifying an appropriate filter constant, effective control can be achieved. However, it is essential to determine the optimal filter constant value by considering the trade-off between response performance and robustness to noise.

Generally, a higher filter constant λ, results in slower response times but increases stability due to robustness against model mismatches. Conversely, a lower λ leads to faster response times but may cause overshoot due to noise from model inaccuracies [20].

The steady-state control output for an oxygen concentration of 4% is analyzed for the five specified controllers, along with the response performance when a step input changes the oxygen concentration from 4% to 5%. By examining the stability of the steady-state at 4% oxygen concentration and the response performance to the step input across the five cases, the optimal filter constant λ can be determined.

The internal model $\bar{\mathcal{G}}_{S2}(s)$ estimated from experimental data may experience discrepancies from the actual plant due to disturbances and changes in environmental variables. Therefore, it is necessary to determine a stable filter constant λ through experimentation to ensure effective control performance in the actual plant. The values of λ for K_p and K_i in Equation 7 can be set between 0.5 and 2.5, as shown in Table 4. Accordingly, five controllers are specified with filter constant values increasing by 0.5 increments, starting from 0.5.

Table 4. Control Gain according to IMC Constant λ of S2 System Controller.

Controller	$\boldsymbol{\lambda}$	$\boldsymbol{K_p}$	$\boldsymbol{K_i}$
$\boldsymbol{C_{br1}}$	0.5	17.265	9.147
$\boldsymbol{C_{br2}}$	1.0	8.633	4.573
$\boldsymbol{C_{br3}}$	1.5	5.755	3.049
$\boldsymbol{C_{br4}}$	2.0	4.316	2.287
$\boldsymbol{C_{br5}}$	2.5	3.453	1.829

5.2. Evaluation Methods

To analyze the steady-state response for the target oxygen concentration of 4% across the five cases, the normal distribution of the measured response data is determined, and the mean and variance are calculated. Additionally, to evaluate the response performance for a step input change from 4% to 5% oxygen concentration in each case, the stability index M_p is analyzed using the Integral of Squared Error (ISE) [26].

The M_p represents the maximum peak error in the step response, as represented by Equation 8. This generally indicates the maximum overshoot before the system reaches a steady state. This metric allows for the comparison of the maximum magnitude of overshoot across different controllers.

$$M_p = max|e(t)| \tag{8}$$

The Integral of Squared Error (ISE) is calculated by integrating the square of the error over time, as represented by Equation 9. This approach amplifies the impact of larger errors by squaring them, allowing for a more significant reflection of their effects. This metric enables the comparative evaluation of overall stability during the transient response period.

$$ISE = \int_{t_s}^{t_f} |e(t)|dt \tag{9}$$

 doi:10.20944/preprints202407.2201.v1

5.3. Steady-State Response

To apply the optimal IMC-PI control parameters to the proposed OFB combustion improvement system $S2$, experimental characteristics are compared. The experiments are conducted with a constant fuel supply of 131 kg/h to the OFB, and the S1 process is halted to measure the standalone performance of $S2$.

Figure 8 presents the experimental results of controlling the oxygen concentration of the OFB system, $\mathcal{P}2$ at 4% for each case. The combustion system $S2$ was controlled for each case, and data was collected for a total of 1200 seconds in the steady state. With a sampling period of 0.25 seconds, the estimation was based on a total of 4800 image data points.

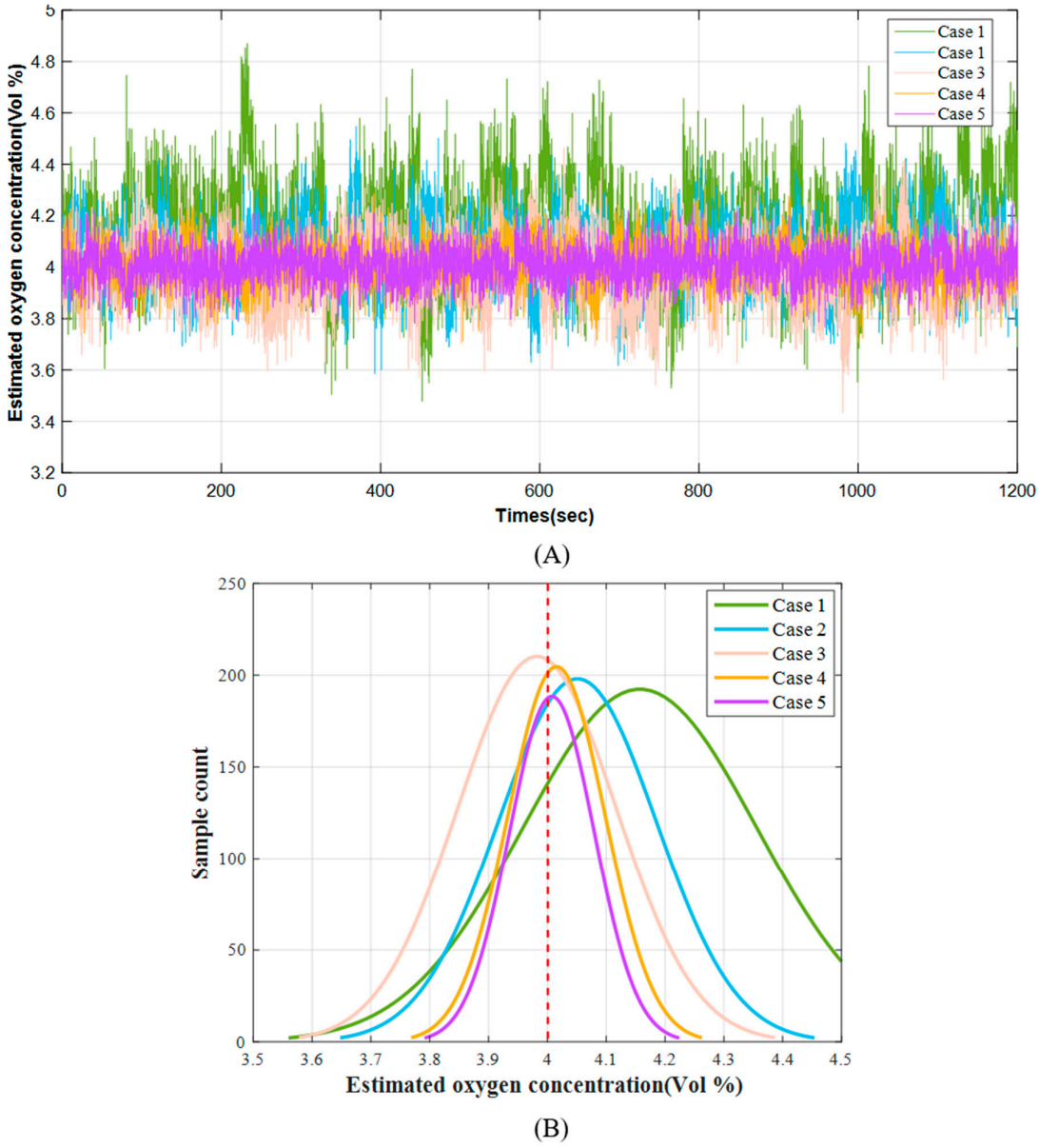

Figure 8. (A) SteadyState Response to Target Oxygen Concentration (B) Normal Distribution of Response Data.

Through this analysis, the mean values for the IMC filter constant λ ranging from 0.5 to 2.5 were found to be 4.1571, 4.0509, 3.9823, 4.0156, and 4.0076, respectively, with variances of 0.0397, 0.0181, 0.0182, 0.0068, and 0.0052.

 doi:10.20944/preprints202407.2201.v1

Figure 8-(A) demonstrates that the control system accurately tracks the target value of 4% for all values of λ. However, it also indicates that as the filter constant λ decreases, the variability around the target value of 4% in the steady state increases.

Figure 8-(B) visualizes the normal distribution of the data collected in the steady state. When λ is 0.5, the steady-state values show a significant error from the target value of 4%, greatly reducing control stability. Conversely, as the value of λ increases, both the steady-state error and variance decrease, indicating improved stability of the control system. These results suggest that increasing the filter constant λ is advantageous for accurate tracking of the target value and maintaining control stability.

5.4. Transient Response Comparison for Step Input

To verify the response performance of the controller, a step change is applied to the control setpoint, and the corresponding step response is observed. The experimental results are shown in Figure 9, and Table 5 presents the performance evaluation based on the filter constant λ.

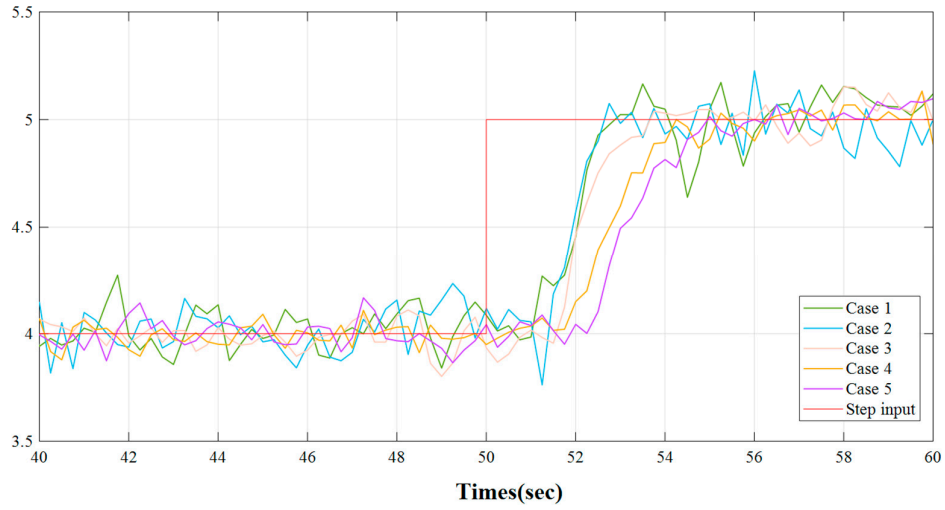

Figure 9. Response by Case to Oxygen Concentration Target Value Step Changes.

Table 5. Response by case to oxygen concentration target value step change.

Controller	4% > 5% Transient Response Comparison		
	λ	M_p	ISE
C_{br1}	0.5	0.377	10.9183
C_{br2}	1.0	0.3579	10.1689
C_{br3}	1.5	0.19245	10.1159
C_{br4}	2.0	0.15869	13.6268
C_{br5}	2.5	0.13824	14.2537

Examining the transient response period from 50 to 56 seconds allows us to assess the control response performance to the step input. In Case 1, with a filter constant λ of 0.5, the transient response is significant, resulting in an M_p of 0.377, and the system exhibits oscillations. In Case 2, with an increased λ, the value of M_p is 0.3579; although the system's oscillations are dampened, the transient response remains unimproved. However, from Case 3 onwards, the M_p significantly improves to 0.19245, and the system no longer oscillates. The ISE represents the error between the target value of 5% and the actual response from 50 to 56 seconds. In Cases 1 to 3, as shown in the graph in Figure 9, the response speeds are similar, resulting in comparable ISE values. However, from

 doi:10.20944/preprints202407.2201.v1

Case 4 onwards, the response speed drastically decreases, causing the ISE to spike to 13.6268. This indicates that starting from a λ of 2.0, the system exhibits discrepancies with the internal model, rendering it unsuitable as a controller for step responses.

Overall, when the values of λ are 0.5 and 1.0, the response speed is faster, but the system experiences oscillations and significant transient responses. At λ is 1.5, although the M_p is slightly higher than in cases 4 and 5, it ensures adequate control response speed without causing oscillations. Additionally, it shows the lowest error in ISE. Therefore, for efficient control of the OFB combustion system, the optimal parameter is achieved by selecting the values of λ as 1.5, as indicated in Case 3.

6. Conclusion

This study proposes and validates a new control system to optimize the combustion process of marine oil-fired boilers, aiming to reduce emissions and increase efficiency. The proposed system uses an SEF and an SVM model to predict oxygen concentration, which is then utilized as an input for an IMC based PI controller. The major findings and contributions of this study can be summarized as follows.

By analyzing flame images in real-time, the proposed system overcomes the measurement delays associated with traditional gas measurement methods, enabling faster and more accurate control of the combustion process. To address the combustion instability caused by transient responses during control, the study proposed and validated system $S2$, which allows for additional adjustments to the air supply while ensuring the combustion stability of the existing proportional combustion control system $S1$. For effective control of this system, obtaining an accurate internal model is essential. Therefore, machine learning-based model estimation methods were employed to calculate the internal model, which is crucial for designing an effective combustion control system. This internal model, estimated through machine learning-based training on experimental input-output data, demonstrates responses similar to the actual system.

However, even though the prediction model based on flame images may exhibit high accuracy, prediction errors can still occur. These errors can arise due to factors such as the model's generalization ability, data noises, and environmental changes, leading to discrepancies between the predicted and actual values in the real system. Consequently, it is important to optimize control stability and performance through the experimental tuning of the IMC-based PI controller. Extensive experimentation revealed that an IMC filter constant (λ) of 1.5 best balances responsiveness and stability, minimizing both overshoot (M_p) and integral of squared error (ISE). This demonstrates that the IMC-based PI controller, using flame images as input, must consider the non-linearities caused by prediction errors, even when the internal model of the system is accurately estimated. Through experimental tuning of the IMC controller, a robust controller can be designed to withstand prediction errors and disturbances.

In conclusion, the implementation of the proposed system combined with real-time IMC-based PI control using flame images offers a feasible and effective solution for enhancing the environmental performance of OFB. This approach can improve combustion efficiency, reducing emissions of harmful air pollutants, and can be easily applied to existing ships, contributing to more sustainable marine air pollution reduction. Furthermore, the ease of installation can encourage participation from shipping companies.

The focus of future research will be designing an intelligent control system for the proposed system that uses flame images as input, with high adaptability to environmental changes and effective control of nonlinear systems. The goal is to enhance combustion efficiency and minimize emissions of air pollutants. In particular, efforts will be made to further strengthen the current system's ability to overcome the nonlinearities caused by prediction errors and to develop adaptive control methods that continuously improve over time.

By advancing the proposed system and integrating it into the combustion system $S2$, as described in this paper, future studies will aim to evaluate its applicability in real marine environments and achieve optimal performance.

Author Contributions: Conceptualization, C.M. Lee., B.G. Jung; methodology, C.M. Lee.; formal analysis, C.M. Lee; writing—original draft preparation, C.M. Lee.; writing—review and editing, J.H Choi.

Funding: The author(s) received no financial support for the research, authorship, and/or publication of this article.

Institutional Review Board Statement: Not applicable.

Informed Consent Statement: Not applicable.

Data Availability Statement: No applicable.

Acknowledgments: First and foremost, we extend our deepest gratitude to everyone who has played a role in the successful completion of this journal. We also wish to express our sincere thanks to the esteemed reviewers for their meticulous evaluation, insightful feedback, and expert guidance throughout the peer review process. Lastly, we are immensely thankful to the editors for their dedication, hard work, and commitment to advancing knowledge in our field

Conflicts of Interest: The author(s) declared no potential conflicts of interest with respect to the research, authorship, and/or publication of this article.

References

1. Das, C.K.; Bass, O.; Kothapalli, G.; Mahmoud, T.S.; Habibi, D. Overview of energy storage systems in distribution networks: Placement, sizing, operation, and power quality. *Renewable and Sustainable Energy Reviews* **2018**, *91*, 1205-1230.
2. Issa, M.; Ilinca, A.; Ibrahim, H.; Rizk, P. Maritime autonomous surface ships: Problems and challenges facing the regulatory process. *Sustainability* **2022**, *14*, 15630.
3. Huang, J.; Duan, X. A comprehensive review of emission reduction technologies for marine transportation. *Journal of Renewable and Sustainable Energy* **2023**, *15*.
4. Walker, T.R.; Adebambo, O.; Del Aguila Feijoo, M.C.; Elhaimer, E.; Hossain, T.; Edwards, S.J.; Morrison, C.E.; Romo, J.; Sharma, N.; Taylor, S.; Zomorodi, S. Chapter 27 - Environmental Effects of Marine Transportation. In *World Seas: An Environmental Evaluation (Second Edition)*; Sheppard, C., Ed.; Academic Press: 2019; pp. 505-530.
5. Liang, X.; Wang, Y.; Chen, Y.; Deng, S. Advances in emission regulations and emission control technologies for internal combustion engines. *SAE International Journal of Sustainable Transportation, Energy, Environment, & Policy* **2021**, *2*, 101-119.
6. Bakalov, I. Constructive solutions to reduce the NOx and SOx in the marine boiler burners. *Trans Motauto World* **2016**, *1*, 7-9.
7. Ragland, K.W.; Bryden, K.M. *Combustion engineering*, CRC press: 2011;.
8. Gaba, A.; Iordache, S.F. Reduction of air pollution by combustion processes. The Impact of Air Pollution on Health, Economy, Environment and Agricultural Sources; InTech: London, UK **2011**, 119-142.
9. Oland, C.B. Guide to low-emission boiler and combustion equipment selection, The Laboratory Oak Ridge, TN, USA: 2002;.
10. Wang, Y.F.; Wang, M.X.; Liu, Y.; Yin, L.; Zhou, X.R.; Xu, J.F.; Zhang, X.Y. Fuzzy modeling of boiler efficiency in power plants. *Inf Sci* **2021**, *542*, 391-405, DOI 10.1016/j.ins.2020.06.064. Available online: https://www.sciencedirect.com/science/article/pii/S0020025520306526.
11. Nemitallah, M.A.; Nabhan, M.A.; Alowaifeer, M.; Haeruman, A.; Alzahrani, F.; Habib, M.A.; Elshafei, M.; Abouheaf, M.I.; Aliyu, M.; Alfarraj, M. Artificial intelligence for control and optimization of boilers' performance and emissions: A review. *J Clean Prod* **2023**, *417*, 138109, DOI 10.1016/j.jclepro.2023.138109. Available online: https://www.sciencedirect.com/science/article/pii/S0959652623022679.
12. Annaswamy, A.M.; Ghoniem, A.F. Active control of combustion instability: Theory and practice. *IEEE Control Syst Mag* **2002**, *22*, 37-54.
13. Kurniawan, E.D.; Effendy, N.; Arif, A.; Dwiantoro, K.; Muddin, N. Soft sensor for the prediction of oxygen content in boiler flue gas using neural networks and extreme gradient boosting. *Neural Computing and Applications* **2023**, *35*, 345-352.
14. Li, S.; Wang, Y. Performance assessment of a boiler combustion process control system based on a data-driven approach. *Processes* **2018**, *6*, 200.

 doi:10.20944/preprints202407.2201.v1

15. Docquier, N.; Candel, S. Combustion control and sensors: a review. *Progress in energy and combustion science* **2002**, *28*, 107-150.
16. Chen, J.; Chang, Y.; Cheng, Y.; Hsu, C. Design of image-based control loops for industrial combustion processes. *Appl Energy* **2012**, *94*, 13-21, DOI 10.1016/j.apenergy.2011.12.080. Available online: https://www.sciencedirect.com/science/article/pii/S0306261911008865.
17. Brown, B.R. Engineering intelligent systems: Systems engineering and design with artificial intelligence, visual modeling, and systems thinking, John Wiley & Sons: 2022;.
18. Ogata, K.; Yang, Y. *Modern control engineering,* Prentice hall India: 2002;.
19. Åström, K.J.; Hägglund, T. *Advanced PID control,* ISA-The Instrumentation, Systems and Automation Society: 2006;.
20. Shamsuzzoha, M.; Lee, M. PID controller design for integrating processes with time delay. *Korean Journal of Chemical Engineering* **2008**, *25*, 637-645.
21. Lee, C.; Jung, B.; Choi, J. Experimental Study on Prediction for Combustion Optimal Control of Oil-Fired Boilers of Ships Using Color Space Image Feature Analysis and Support Vector Machine. *Journal of Marine Science and Engineering* **2023**, *11*, 1993.
22. García, A.C.; Alban, C.A.P.; Benalcázar, J.R.T.; Rodríguez, A.C.; Lorente-Leyva, L.L.; Aleaga, A.M.L. Control of Pollutant Emissions from a Boiler Through the Percentage of Oxygen. *Journal Européen des Systèmes Automatisés* **2021**, *54*, 469-474.
23. Chen, J.; Chang, Y.; Cheng, Y. Performance design of image-oxygen based cascade control loops for boiler combustion processes. *Ind Eng Chem Res* **2013**, *52*, 2368-2378.
24. Xiao, G.; Gao, X.; Lu, W.; Liu, X.; Asghar, A.B.; Jiang, L.; Jing, W. A physically based air proportioning methodology for optimized combustion in gas-fired boilers considering both heat release and NOx emissions. *Appl Energy* **2023**, *350*, 121800.
25. Li, Y.; Zhang, T.; Das, S.; Shamma, J.; Li, N. Non-asymptotic System Identification for Linear Systems with Nonlinear Policies. *IFAC-PapersOnLine* **2023**, *56*, 1672-1679.
26. Goodwin, G.C.; Graebe, S.F.; Salgado, M.E. *Control system design,* Prentice Hall Upper Saddle River: 2001;.